RESEARCH ARTICLE

# A Comparative Transcriptomic Analysis of Development in Two *Astyanax* Cavefish Populations

JOURNAL OF EXPERIMENTAL ZOOLOGY PART B MOLECULAR AND DEVELOPMENTAL EVOLUTION

BETHANY A. STAHL AND JOSHUA B. GROSS*
Department of Biological Sciences, University of Cincinnati, Cincinnati, Ohio

**ABSTRACT**

Organisms that are isolated into extreme environments often evolve extreme phenotypes. However, global patterns of dynamic gene expression changes that accompany dramatic environmental changes remain largely unknown. The blind Mexican cavefish, *Astyanax mexicanus*, has evolved a number of severe cave-associated phenotypes including loss of vision and pigmentation, craniofacial bone fusions, increased fat storage, reduced sleep, and amplified nonvisual sensory systems. Interestingly, surface-dwelling forms have repeatedly entered different caves throughout Mexico, providing a natural set of "replicate" instances of cave isolation. These surrogate "ancestral" surface-dwelling forms persist in nearby rivers, enabling direct comparisons to the "derived" cave-dwelling form. We evaluated changes associated with subterranean isolation by measuring differential gene expression in two geographically distinct cave-dwelling populations (Pachón and Tinaja). To understand the impact of these expression changes on development, we performed RNA-sequencing across four critical stages during which troglomorphic traits first appear in cavefish embryos. Gene ontology (GO) studies revealed similar functional profiles evolved in both independent cave lineages. However, enrichment studies indicated that similar GO profiles were occasionally mediated by different genes. Certain "master" regulators, such as *Otx2* and *Mitf*, appear to be important loci for cave adaptation, as remarkably similar patterns of expression were identified in both independent cave lineages. This work reveals that adaptation to an extreme environment, in two distinct cavefish lineages, evolves through a combination of unique and shared gene expression patterns. Shared expression profiles reflect common environmental pressures, while unique expression likely reflects the fact that similar adaptive traits evolve through diverse genetic mechanisms. *J. Exp. Zool. (Mol. Dev. Evol.) 328B:515–532, 2017.* © 2017 Wiley Periodicals, Inc.

*J. Exp. Zool. (Mol. Dev. Evol.) 328B:515–532, 2017*

**How to cite this article: Stahl BA, Gross JB. 2017. A comparative transcriptomic analysis of development in two *Astyanax* cavefish populations. J. Exp. Zool. (Mol. Dev. Evol.) 328B:515–532.**

The dark and nutrient-poor cave environment has become home to a diverse array of taxa. Many cave-adapted organisms have thrived in this extreme environment; however, the genetic changes governing their success have remained largely unknown. The recurrent evolution of certain stereotypical phenotypes, such as eye/pigmentation loss and nonvisual sensory expansion, suggests that selection is driving the evolution of these phenotypes across different cave biomes (Jeffery, 2001).

Bethany A. Stahl's current address: Department of Biological Sciences, Florida Atlantic University, Jupiter, Florida.
Grant sponsor: US National Science Foundation; Grant number: DEB-1457630; Grant sponsor: US National Institutes of Health (NIDCR); Grant number: R01DE025033.

Additional Supporting Information may be found in the online version of this article.
*Correspondence to: Joshua B. Gross, Department of Biological Sciences, University of Cincinnati, Cincinnati, OH 45221.
Email: grossja@ucmail.uc.edu
Received 15 December 2016; Revised 24 March 2017; Accepted 11 April 2017
DOI: 10.1002/jez.b.22749
Published online 14 June 2017 in Wiley Online Library (wileyonlinelibrary.com).

However, neutral mutation may also participate as a mechanism driving trait degeneration (Wilkens, '88) based on the presence of deleterious mutations found in various key pigmentation genes (Protas et al., 2006; Gross et al., 2009).

The blind Mexican cavefish, *Astyanax mexicanus*, comprises both surface-dwelling forms and numerous independently derived cave adapted populations (Jeffery, 2001). Population genetic studies suggest a complex evolutionary history resulting from several cave invasions of "old" and a "young" stocks of surface-dwellers that invaded NE Mexico, ~2–5 My and ~1–2 My, respectively (Bradic et al., 2012; Gross, 2012). This demographic history provides the opportunity to understand global genetic changes accompanying *repeated* isolation into the subterranean environment.

Data from prior studies do not uniformly support a universal mechanism underlying cavefish isolation into subterranean caverns. For instance, complementation studies between different eyeless populations resulted in offspring with functional visual systems (Wilkens and Strecker, 2003; Borowsky, 2008). This implied that different cave populations produce the same eye-loss phenotype through different sets of genes. Conversely, certain Mendelian traits (albinism and *brown*) are caused by mutations to the same genes (*Oca2* and *Mc1r*) in geographically distinct populations (Protas et al., 2006; Gross et al., 2009). These disparate results beg the question of whether repeated cave adaptation evolves principally through changes to the same sets of genes or distinct genetic mechanisms.

A historical lack of genomic resources in *Astyanax* limited prior analyses to candidate gene studies. The recent availability of a draft *Astyanax* genome enables comprehensive quantification of genome-wide expression patterns in both morphotypes (McGaugh et al., 2014). Using a genomic reference template, we performed mRNA-sequencing (RNA-seq) to directly compare transcript abundance between surrogate "ancestral" surface fish and two independent cave populations, Pachón and Tinaja (Fig. 1). Both caves are in the same "El Abra" region, but each was inhabited independently by subpopulations of the "older" stock of surface-dwelling fish (Bradic et al., 2012). Since many phenotypic differences between surface and cavefish emerge throughout the first ~96 hr of development (Jeffery, 2009b), we profiled expression at four embryonic time points within this critical window to capture expression differences associated with these dynamic morphological changes.

In this analysis, we discovered unexpectedly diverse patterns of expression. For instance, Tinaja and Pachón cavefish demonstrated distinct transcriptomic responses to cave adaptation—Tinaja cavefish harbored more upregulated genes than Pachón cavefish. Conversely, Pachón cavefish demonstrate nearly twice as many downregulated genes compared to Tinaja. Gene ontology (GO) term enrichment analyses revealed a complex pattern of both shared and divergent gene processes in each cave population. Interestingly, several "shared" GO term functions were associated with different genes in the two cave populations, suggesting selection for certain phenotypes occurs at the level of gene function during cave adaptation.

Further, a bioinformatic pathway analysis revealed similar levels of expression change for the genes *Otx2* and *Mitf* in both cave lineages. Thus, certain "master regulator genes" may be intimately linked to the process of cave adaptation. Shared patterns of gene expression echo similarities in environmental pressures of the two cave microenvironments (e.g., reduced light and nutrition). Divergent expression patterns, however, may reflect more subtle ecological differences between Pachón and Tinaja, or demographic differences (timing of isolation, migration rates) between the two populations. Additional natural history and population genetic studies will further clarify the precise environmental pressures and degree of relatedness between different populations. This information will augment our ability to understand these global transcriptomic changes (both similarities and differences) in the context of the natural cavefish landscape. Collectively, this work reveals a complex transcriptomic response to cave adaptation in two ancient cave lineages that appears to evolve through a mosaic of shared and divergent genes and gene functions, as well as certain crucial "cave-associated" genes.

## MATERIALS AND METHODS

### Animal Husbandry and Rearing

Adult surface, Pachón and Tinaja cavefish were reared in a custom husbandry unit (Aquaneering, San Diego, CA) equipped with automatic dosers to control pH (~7.4 ± 0.2) and conductivity (~800 ± 50 $\mu$S/m) levels. Animals were maintained under a stable 12 hr light:12 hr dark cycle at ~24°C in 10-gallon glass tanks. Adults were fed a standard diet of TetraMin Pro flake food. One week prior to breeding, adults were fed a diverse diet of liver paste, frozen blood worms, frozen *Daphnia*, frozen brine shrimp, live black worms, and live *Daphnia*. Natural breedings were induced from groups of three to six adults with an overnight increase (+2–3°C) in tank water temperature, following 2 days of increased feeding and diversity of nutrition. Breeding groups typically included more males than females. *Astyanax mexicanus* is an emerging model system, and therefore are more challenging to breed in captivity compared to "traditional" model systems (e.g., zebrafish). To address this challenge, we pooled clutches of same-staged individuals from multiple group breedings to achieve a collective representative set of four developmental stages (below). We extensively profiled a single RNA pool, in technical triplicate (see below), to control for variability between sequencing runs. This approach enabled us to reduce interindividual genotypic variability in order to focus on expression differences across the *Astyanax* transcriptome. All adult fish were generously provided by Dr. Richard Borowsky (New York University). All procedures involving animal were performed in accordance with the ethical standards

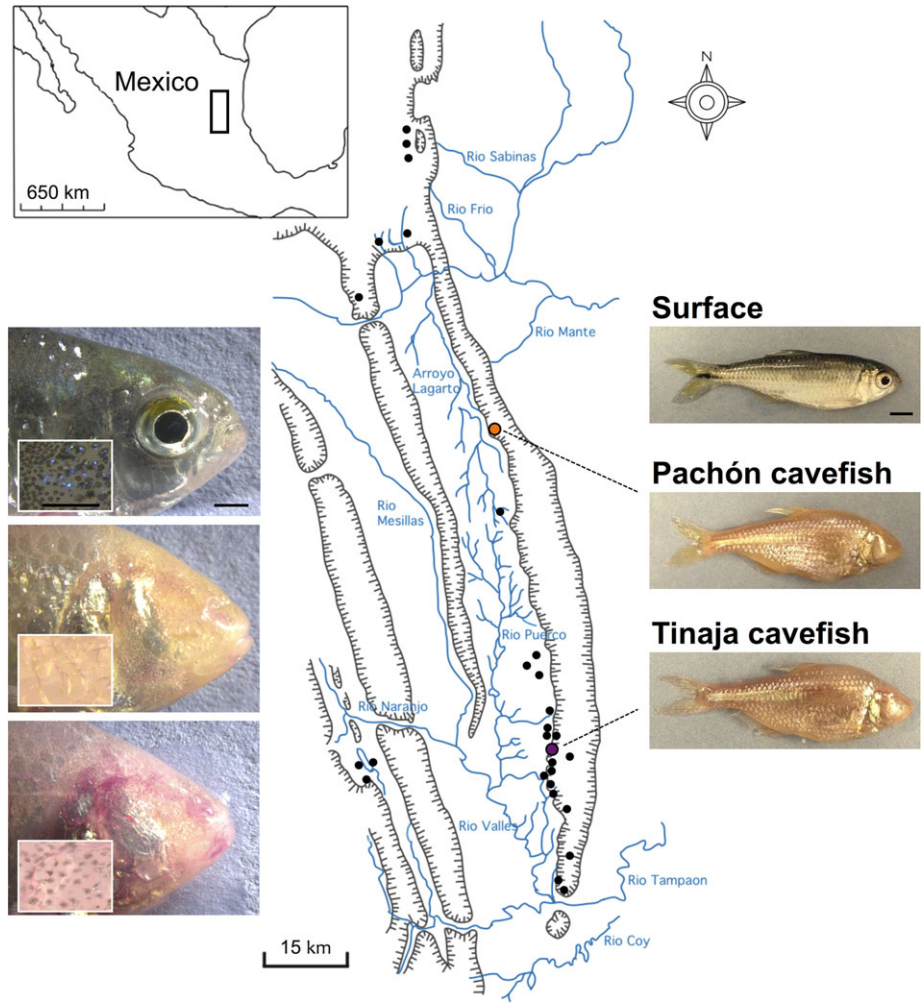


**Figure 1.** Two geographically isolated *Astyanax* cavefish populations. To characterize gene expression changes associated with cave isolation, we utilized cavefish derived from two independent lineages—Pachón and Tinaja localities—to compare with surface-dwelling from nearby rivers and streams throughout the El Abra region of northeastern Mexico (whole body images, right panels). Fish from the Pachón and Tinaja caves appear quite similar; however, higher magnification reveals clear differences between individuals. For example, Pachón cavefish harbor albinism (complete absence of pigmentation), yet Tinaja cavefish maintain a low level of melanin coloration, which is severely reduced compared to surface fish (head and dorsal square inset, left panels). Scale bars = 0.5 cm. [Color figure can be viewed at wileyonlinelibrary.com]

of the National Institutes of Health Guidelines under a protocol approved by the Institutional Animal Care and Use Committee of the University of Cincinnati (Protocol Number 10-01-21-01).

### mRNA Extraction and Purification

Embryos were reared to the appropriate embryonic stage according to the *Astyanax* developmental staging series in clean system water (Hinaux et al., 2011). RNA pools were isolated for surface fish, Pachón cavefish, and Tinaja cavefish for the following four stages: 10 hr postfertilization (hpf), 24, 36, and 72 hpf. At the 10 hpf stage, *Astyanax* embryos are beginning somitogenesis, and the 24 hpf stage represents the end of somitogenesis (Hinaux et al., 2011). By the 36 hpf developmental stage, the pectoral fin bud has emerged, and at the 72 hpf stage, the jaws have begun formation (Hinaux et al., 2011). Under sterile conditions, 50 embryos were collected from each developmental stage and pooled for RNA extraction, according to manufacturer recommendations (RNeasy Plus Mini Kit; Cat. No. 74134; Qiagen, Germantown, MD). Each pool was passed through a genomic DNA "eliminator" column to render a pure extract of total RNA.

Following purification, all samples were immediately quantified and assessed for RNA quality (A260/280 ratio ~2.0–2.1) using a NanoVue Plus Spectrophotometer (GE Healthcare, Chicago, IL, Product No. 28-9569-62). Samples were diluted to a final concentration of 40 $\mu$g/mL in 50 $\mu$L of RNAse-free water, and stored at –80°C until sample submission.

### mRNA Sequencing

RNA sequencing was carried out at the Cincinnati Children's Hospital Medical Center DNA Sequencing and Genotyping Core (http://dna.cchmc.org) using an Illumina Hi-Seq 2500 sequencing instrument. Libraries were generated from ~1 $\mu$g of purified total RNA using the Illumina TruSeq (v.2) kit. All RNA samples were checked for, and passed, the CCHMC Core quality threshold prior to library preparation. Samples were sequenced for ~10 million (single-end, 50-bp) reads. Each developmental stage was subdivided into three separate samples that were each sequenced in technical triplicate. In total, we performed 36 RNA sequencing experiments: four developmental stages (each sequenced in triplicate) for surface fish, Pachón cavefish, and Tinaja cavefish. Following sequencing, raw data were retrieved (fastq-formatted files) and used for subsequent sequence alignment and expression analyses. Surface fish and Pachón cavefish sequencing reads were shared in advance of publication to augment the available resources for the *Astyanax* genome project (McGaugh et al., 2014) and are available through the NCBI Sequence Reads Archive under BioProject accession #PRJNA258661. Tinaja cavefish sequencing reads have been deposited under the same BioProject ID (#PRJNA258661).

### RNA-seq Expression Analyses

RNA-sequencing reads from each of four developmental stages (10, 24, 36, and 72 hpf in triplicate) were aligned to the draft *Astyanax* genome template (Ensembl Genome Browser v.75) comprising a comprehensive set of predicted cDNA sequences ($n$ = 23,719). The raw sequencing reads derived from 36 fastq files were imported into ArrayStar (DNAStar.v.12.0, Madison, WI) and aligned to the *Astyanax* global cDNA template. Replicate sequencing runs were grouped and normalized read counts were calculated for surface, Pachón cavefish, and Tinaja cavefish at each of the four time points using the RPKM normalization strategy (9) in ArrayStar (DNAStar.v.12.0; see Gross et al., 2013). This normalization approach accounted for differences in gene length, variation in the depth of each sequencing run, and reads aligning to more than one cDNA template sequence (Mortazavi et al., 2008). This software package has been widely accepted for analysis of RNA-sequencing data (Leyva-Pérez et al., 2014; Guaiquil et al., 2014). Expression differences (fold change) were determined for every gene across development in each cavefish population ("experimental") relative to the surrogate "ancestral" surface-dwelling form ("control"; ArrayStar, DNASTAR.v.12.0) (Mortazavi et al., 2008). The significance of differential expression for each gene comparison was determined using a Student's $t$-test with FDR (Benjamini and Hochberg, 2000) using ArrayStar (DNASTAR.v.12.0; see Supplementary Table S1). This Student's $t$-test, a widely used approach to identify differentially expressed genes, was implemented to compare the mean gene expression value (derived from replicate sequencing) between each of two groups (cave population vs. surface fish population) for a given gene. ArrayStar software utilizes an unpaired, two-tailed, equal variance Student's $t$-test. Genes of predicted biological relevance for cave-associated phenotypes were further analyzed if they reached a significance level of 0.05 or 0.10 (FDR adjusted $P$-value; DNASTAR.v.12.0), consistent with other RNA-seq reports (Warden et al., 2013; Love et al., 2014; Seo et al., 2016).

All downstream analyses stemmed from the pairwise transcriptomic comparisons (Pachón cavefish vs. surface fish; Tinaja cavefish vs. surface fish). However, we focused on the most extreme differences in expression that were either shared or unique to each cavefish population. We set a threshold for further evaluating expression differences as those genes expressed at ≥ 10-fold in each cavefish lineage compared to surface fish. This threshold yielded the following data set: Pachón ($n$ = 1,248 genes) and Tinaja ($n$ = 1,776 genes). We then compared gene identities at each of four developmental stages in each data set (Pachón vs. Tinaja) using Ensembl transcript IDs. We defined "convergent" expression as genes with matching transcript IDs that reached the ≥ 10-fold threshold at a given time point in both cavefish populations. Conversely, genes expressed at ≥ 10-fold difference in only one cavefish lineage were defined as "divergent" in expression.

To mitigate the concern for reduced biological variability in our RNA samples, we also performed expression-level validation for a number of representative genes (see Results section). cDNA pools utilized for this validation step were drawn from at least five different lines of each morphotype from diverse pedigrees and individuals. In total, four developmental stages were isolated for each of three morphotypes (Pachón cavefish, Tinaja cavefish, and surface fish) comprised of several different pedigrees that were derived from the natural cave and surface populations.

### GO Enrichment Analysis

GO enrichment studies were carried out using Blast2GO v.2 (www.blast2go.com). We evaluated multiple thresholds to estimate an appropriate number of overexpressed (+) and underexpressed (–) genes in Pachón and Tinaja cavefish compared to surface fish. Since each cave population demonstrated different numbers (and fold-change levels) of overexpressed and underexpressed genes, we defined a set number of genes for comparison. This approach enabled us to directly compare the "most" overexpressed or underexpressed genes in each cave population, irrespective of minor differences in the level of expression. These thresholds included the top 1%

($n = 237$), 2.5% ($n = 592$), 5% ($n = 1,185$), and 10% ($n = 2,371$) differentially expressed genes. For each percent threshold, genes were collated and assembled into "test sets," and enrichment of terms in each set were determined through comparison with all ontology terms in the *Astyanax* genome (v.75) reference, using Fischer's exact test ($P < 0.05$; Blast2GO). The 2.5% threshold ($n = 592$ genes) provided the most biologically informative terms for downstream analyses (see Supplementary Table S2).

### Qualitative and Quantitative PCR Validation

A subset of gene expression patterns observed in RNA-seq studies were confirmed using quantitative PCR (described in Gross and Wilkens, 2013). Total RNA free of genomic DNA contamination was prepared from stage-matched Pachón ($n = 50$), Tinaja ($n = 50$), and surface fish ($n = 50$) embryos at 72 hpf using the RNeasy extraction kit (Qiagen). cDNA templates were synthesized from 1 $\mu$g of high-quality RNA annealed with oligo dT primers (Invitrogen) at 65°C for 10 min. After cooling for 5 min on ice, a mixture of 4 $\mu$L 5 × RT buffer, 0.5 $\mu$L protector RNase inhibitor, 2 $\mu$L dNTP mixture and 0.5 $\mu$L Transcriptor RT was added to each reaction, incubated at 50 °C for 1 hr, and then inactivated at 85°C for 5 min. We note that cDNA pools used for validation were drawn from at least five different group breedings to determine the degree to which biological variability may skew the results we obtained from RNA-sequencing. Of note, RNA pools utilized for qPCR validation are distinct biological samples from the pools sequenced. For the representative set of genes that were profiled, we found highly consistent results despite having been evaluated across a diverse set of cDNA pools.

We amplified six test genes in sextuplet across using a MiniOpticon light cycler (Bio-Rad, Hercules, CA). Quantification cycle ($C_q$) values were determined from each sample and normalized by comparison to the reference gene *ribosomal protein s18* (*Rps18*; ENSAMXT00000008147) (primers: forward = 5′-ACACGAACATCGATGGTAGGAG-3′, reverse = 5′-TTGTTGAGGTCGATGTCTGC-3′, 112 bp; (McCurley and Callard, 2008). Experimental gene primer sets included *slc5a8* (ENSAMXT00000021731) (forward = 5′-AGGCACACTTTCTGGACTATCC-3′, reverse = 5′-AACAGGGACTTGCAAGACAC-3′, 107 bp); *Or115-15* (ENSAMXT00000025780) (forward = 5′-CAGCGGTTTTACTTGGATCTTCC-3′, reverse = 5′-TGCTGCAGGTTTTCAAAGCC-3′, 120 bp); *itln1* (ENSAMXT00000003604) (forward = 5′-AACCGGGCTACATTTGGAAC-3′, reverse = 5′-TTATTGGGAACGTGCCACAC-3′, 110 bp); *sb:cb1081* (ENSAMXT00000018849) (forward = 5′-GCAGCAGCTGTTTGCATATG-3′, reverse = 5′-AAGCCAAGGAAGAAGGAAGC-3′, 99 bp); and *Or101-1* (ENSAMXT00000025777) (forward = 5′- GAACCGACTCCAAGCTGAATTC -3′, reverse = 5′- TGAAAGCATGTTGGGGACTG -3′, 101 bp). Primer sets amplified fragments using EvaGreen Supermix dye (Bio-Rad) using the following cycling parameters: step 1: 95°C for 30 sec, step 2: 95°C for 5 sec, step 3: 55.1°C for 10 sec, plate read, repeat step 2 for 39 additional cycles. qPCR data were collected and analyzed for normalized fold expression values ($\Delta\Delta C_q$) using Bio-Rad CFX Manager v.3.1 software (Bio-Rad). Qualitative expression was also measured using routine PCR on pooled 72 hpf cDNA libraries (described above). The gene *Rps18*, *ribosomal protein S18*, was used as an internal standard for all qualitative PCR experiments. We amplified fragments in our target genes ~300–600 bp in length for *Rps18* (forward = 5′-TGGCTGGTTAGATGGGTAGC-3′, reverse = 5′-AGCCCTTGGCGGTTTACTAT-3′, 470 bp), *slc5a8* (forward = 5′-AGATCTCTGGGGAGCTGTGA-3′, reverse = 5′-GGCATTAGCTGGTCTTGAGC-3′, 492 bp), *Or115-15* (forward = 5′-CAGTGGAAAGGAACCTGCAT-3′, reverse = 5′-TGTGCTGCAGGTTTTCAAAG-3′, 584 bp), *itln1* (forward = 5′-CTACCTGACAACGGAGAGTGG-3′, reverse = 5′-GTCTCGGCGTTATTGGGAAC-3′, 306 bp), *sb:cb1081* (forward = 5′-CCTCACTGAGCACACCAAGA-3′, reverse = 5′-GCTGGAGCAGGAGTTACAGG-3′, 643 bp), and *Or101-1* (forward = 5′-AGAACCGACTCCAAGCTGAA-3′, reverse = 5′-GCTGATGGCTTTCCCAATTA-3′, 531 bp). Bands were visualized using standard (2%) gel electrophoresis under UV transillumination.

### Ingenuity Pathway Analysis

We performed an ingenuity pathway analysis (IPA; Qiagen.v.1.0; www.ingenuity.com/products/ipa) to uncover relevant functions and pathways in our global RNA-seq data set. The IPA analysis package only provides annotation for a few mammalian genomes, so all *Astyanax* Ensembl transcript IDs were converted to the corresponding human, mouse, or rat Ensembl protein orthologs using BioMart (www.ensembl.org/biomart/). Using these identifiers, the output from our RNA-seq analysis was then uploaded (see Methods section; fold change and *P*-value for each population—Pachón and Tinaja relative to surface—by developmental stage) using the "flexible format" utilizing default settings and a fold change cutoff of 2.0.

We implemented the "IPA Upstream Regulator" tool, which predicts prospective gene regulators based upon two statistical measures. The first "overlap *P*-value" identifies any statistically significant overlap between the observed expression changes in our RNA-seq data set and genes known to be governed by the regulator (from the Ingenuity® Knowledge Base) using Fisher's exact test ($P < 0.01$; IPA Qiagen.v.1.0). We utilized a second metric, the "activation z-score," which quantifies the regulation direction (i.e., activating or inhibiting). This information is based on relationships and experimentally observed results within a given molecular network. Using this combined information, the program predicts the state of the transcriptional regulator. Since some genes within a network can show expression patterns inconsistent with the predictions, the program provides a statistical measure (i.e., an activation z-score) that determines if a regulator has significantly more "activated" predictions than inhibited predictions (*z*-score > 0). Conversely, a regulator that has a predicted inhibition state should have significantly more

"inhibited" downstream targets (*z*-score < 0; IPA Qiagen.v.1.0). These *z*-scores provide a metric for "sorting" each data set to identify upstream genetic regulators most affected and best supported by observed RNA-seq expression changes affecting putative gene targets. Regulators yielding significant results, and their corresponding gene networks, were visualized using the "My Pathway" analysis tool (IPA Qiagen.v.1.0).

## RESULTS AND DISCUSSION

### Cave Adaptation is Mediated by Different Gene Expression Patterns in Two Ancient Cavefish Lineages

Numerous populations of surface-dwelling fish have become isolated in the vast subterranean caverns of northeastern Mexico (Mitchell et al., '77). Since related surface-dwelling fish persist in the rivers and streams surrounding the El Abra cave network, *Astyanax* cavefish provide the opportunity to compare derived cave forms to a surrogate "ancestral" form. The historical literature has revealed numerous changes at the morphological, behavioral, and molecular levels between morphs (Mitchell et al., '77; Jeffery and Strickler, 2003; Strickler and Jeffery, 2009; Pottin et al., 2011; Gross et al., 2013; O'Quin et al., 2013; Kowalko et al., 2013; McGaugh et al., 2014). Two prior transcriptomic analyses have been performed in *Astyanax*. Hinaux et al. (2013) constructed a de novo transcriptome, derived from embryonic and larval RNA pools in cave and surface fish, using Sanger sequencing. This approach revealed a large number of mutations in visual system genes in the cavefish lineage. Gross et al. (2013) generated an integrated transcriptome, derived from adult pools of RNA from cave and surface fish, using next-generation sequencing technology. This study revealed numerous informative SNPs for genetic mapping, and provided insight to the function of uniquely expressed genes in each adult morphotype. In this report, we sought to explore dynamic transcriptomic alterations across development in surface fish and two distinct cave populations.

The El Abra cavefish populations, including Pachón and Tinaja cavefish, are believed to have arisen from the same ancestral surface fish stock in NE Mexico ~3–5 MYa (Gross et al., 2012). Comparisons across the broader landscape have revealed substantial convergence at the level particular genes for traits like albinism (Protas et al., 2006) and reduced melanization (*brown*; Gross et al., 2009). This may indicate adaptation to the extreme cave environment is accomplished through a limited set of genes. To evaluate this question in the context of gene expression changes, we developmentally profiled two independent *Astyanax* cave populations—Pachón and Tinaja—and compared them to extant surface-dwelling fish (Fig. 1). We aligned and quantified reads derived from stage-matched Pachón, Tinaja, and surface embryos at four key developmental stages using a genome-wide template. We discovered substantial differential expression between lineages, including many genes demonstrating >10 fold-level changes in one or both cavefish populations (Pachón or Tinaja) compared to surface fish. However, many genes were also expressed at nearly equivalent levels (less than onefold difference) between cave and surface fish. We determined the "average fold change" across four developmental stages for Pachón cavefish versus surface and Tinaja cavefish versus surface. Interestingly, the majority of genes in both cavefish populations exhibited minimal expression difference relative to surface fish (~19,000 of 24,000 total genes). However, roughly 5,000 genes demonstrated a fold change difference of 2 or greater in each cavefish population (compared to surface fish; Supplementary Table S3). Stringent filtering limited our data set to those genes demonstrating dramatic expression differences in both cave populations: including fourfold (Pachón vs. surface: 2,729; Tinaja vs. surface: 3,352), sixfold (Pachón vs. surface: 1,948; Tinaja vs. surface: 2,553), eightfold (Pachón vs. surface: 1,516; Tinaja vs. surface: 2,080), and 10-fold (Pachón vs. surface: 1,248; Tinaja vs. surface: 1,776).

Compared to surface fish, Pachón and Tinaja cavefish "overexpress" similar numbers of genes at each threshold level: twofold (Pachón vs. surface: 3,000; Tinaja vs. surface: 2,032), fourfold (Pachón vs. surface: 1,536; Tinaja vs. surface: 1,124), sixfold (Pachón vs. surface: 1,087; Tinaja vs. surface: 858), eightfold (Pachón vs. surface: 829; Tinaja: 698), and eightfold (Pachón vs. surface: 683; Tinaja vs. surface: 594). However, Tinaja cavefish demonstrate reduced expression of nearly twice as many genes at each fold change threshold compared to Pachón: twofold (Pachón vs. surface: 2,115; Tinaja vs. surface: 3,674), fourfold (Pachón vs. surface: 1,193; Tinaja vs. surface: 2,228), sixfold (Pachón vs. surface: 861; Tinaja vs. surface: 1,695), eightfold (Pachón vs. surface: 687; Tinaja vs. surface: 1,382), and 10-fold (Pachón vs. surface: 565; Tinaja vs. surface: 1,182; Supplementary Table S4).

Collectively, these data demonstrate that recurrent cave adaptation does not proceed through expression changes affecting identical genes, or identical numbers of genes, in different lineages. Importantly, many of the gene expression differences we observed were likely not present at the time that these two populations were established. Many of the observed transcriptomic alterations we observed most likely accumulated as the two cave populations adapted to the cave environment. Although Tinaja and Pachón cavefish are descended from the "old" El Abra stock of epigean ancestors, Pachón fish are regarded as older and more "troglomorphic" (cave-adapted) compared to Tinaja fish (Gross, 2012). Our results may indicate that cavefish evolving from more recent (and less geographically isolated) cave entry events, such as Tinaja cavefish, may adopt troglomorphic phenotypes more frequently through expression-level changes. In contrast, cavefish from the isolated Pachón locality may lose traits more often through accumulation of loss-of-function (LOF) mutations as a consequence of a longer period of isolation. For instance, Pachón cavefish may harbor more LOF mutations, assuming they have

arisen in response to more extended periods of relaxed selection (Protas et al., 2006; Gross, 2012).

Given the large number of expression differences in both cave forms compared to surface fish, we next evaluated genes demonstrating the most extreme expression changes. We assumed that those genes demonstrating the highly polarized expression patterns would be more crucial for adaptation to the cave environment. We captured all genes differentially expressed ≥ 10-fold (+ or –) at each of four embryonic stages, as well as the mean (fold) expression difference across development. Genes categorized as "convergent" in expression had matching transcript IDs that reached the ≥ 10-fold threshold at a given developmental stage in both cavefish populations. In contrast "divergent" genes were expressed at ≥10-fold difference in only one cavefish lineage at a given developmental stage. Certain orthologous genes were expressed similarly in both lineages; however, many genes were expressed in a divergent (unique), cave-specific fashion (Supplementary Table S2). Of the 10-fold or greater "underexpressed" genes in Pachón ($n = 724$) and Tinaja ($n = 597$) at 72 hpf, 188 genes were shared in both populations. This indicates a substantial level of transcriptomic convergence, at the level of specific genes, in subterranean isolation.

A large number of genes at the 72 hpf stage, however, demonstrated individual cave-specific patterns of expression (≥10-fold) in Pachón ($n = 536$) and Tinaja ($n = 409$). Surprisingly, at 72 hpf, ~30% of differentially genes (≥10-fold) in Pachón and Tinaja showed convergent levels of reduced expression. The remaining genes (~70%) demonstrated divergent expression patterns (Supplementary Table S5). This complex mosaicism of convergence and divergence was observed at all stages of development for both under- and overexpressed genes (Supplementary Tables S2 and S3).

The divergent patterns of gene expression we observed are consistent with results of complementation studies demonstrating that different loci mediate visual system loss in distinct eyeless populations. Alternatively, these divergent expression patterns may reflect different environmental pressures in each cave (e.g., presence/absence of nutrition resulting from bat roosts) that, in turn, could influence the evolution of distinct phenotypes. Gene expression changes associated with different ecological conditions may be manifested during development, explaining differential expression patterns observed at 72 hpf. Although transcriptomic responses are not identical for independent caves, genes of similar function may participate in recurrent adaptation to the cave microenvironment. To evaluate this possibility, we explored ontology terms associated with genes demonstrating extreme differences between cave and surface fish.

### GO Enrichment Reveals Convergence and Divergence for Cave-Associated Traits

We characterized biological functions associated with differentially expressed genes across four stages of development. We tested several thresholds (see Methods section); however, the top 2.5% of over- and underexpressed genes included those with morphological and/or behavioral relevance, and provided a manageable number of genes for further analysis (Stricker and Jeffery, 2009; Gross et al., 2013). GO enrichment analyses (Fig. 2; Supplementary Table S2) revealed a suite of terms associated with well-known regressive (loss of pigmentation, eye reduction, altered circadian rhythms) and constructive changes (metabolic efficiency, acute nonvisual sensation, starvation resistance) affecting troglomorphic animals.

Several cave-associated terms were present in both Pachón and Tinaja enrichment sets. Among those in the "convergent underexpressed" category (Fig. 2, blue), GO terms relating to vision loss are included ("absorption of visible light," "G-protein coupled photoreceptor activity," "photoreceptor outer segment"). Enrichment analyses of overexpressed genes in both populations (Fig. 2, red) revealed GO terms such as "determination of left/right asymmetry in lateral mesoderm" and "sensory perception of taste." These terms are consistent with previous studies reporting evolved differences in lateral craniofacial asymmetry (Gross et al., 2014) and behavioral modifications for feeding (Kowalko et al., 2013) in obligate cave-dwellers.

Genes demonstrating unique reduced expression in Pachón cavefish were enriched for the term "eye pigmentation," consistent with the absence of pigmentation and eyes in this population (Jeffery, 2001, 2005). Among the overexpressed genes unique to Pachón cavefish were a number of metabolism and appetite-related processes (e.g., "adult feeding behavior," "energy reserve metabolic process," "negative regulation of appetite," "cellular response to starvation"). This is consistent with previous studies documenting highly efficient metabolic rates in Pachón cavefish compared to surface fish, as well as other cave populations (Moran et al., 2014, 2015; Aspiras et al., 2015).

The underexpressed gene set in Tinaja included GO terms for "sensory perception of smell," "melanocyte-stimulating hormone receptor activity," "lens fiber cell differentiation," and "lysozyme activity." These "enriched" eye-related terms and functions differed from those identified in Pachón and could indicate that Tinaja cavefish evolved certain cave-associated traits through different genetic changes. Terms derived from the Tinaja uniquely overexpressed gene set included enrichment for "adipose tissue development," "negative regulation of intrinsic apoptotic signaling pathway in response to oxidative stress," and "9,10 (9', 10')-carotenoid-cleaving dioxygenase activity." These results reflect well-characterized cave-associated traits including increased fat content (Aspiras et al., 2015), lens apoptosis during early development (Yamamoto and Jeffery, 2000), and abundance of yellow-orange carotenoids in cave lineages (Culver and Wilkens, 2000).

Convergence in GO terminology did not always signal expression changes in the same genes. For instance, Pachón and Tinaja cavefish data sets were enriched for "detection of chemical stim-

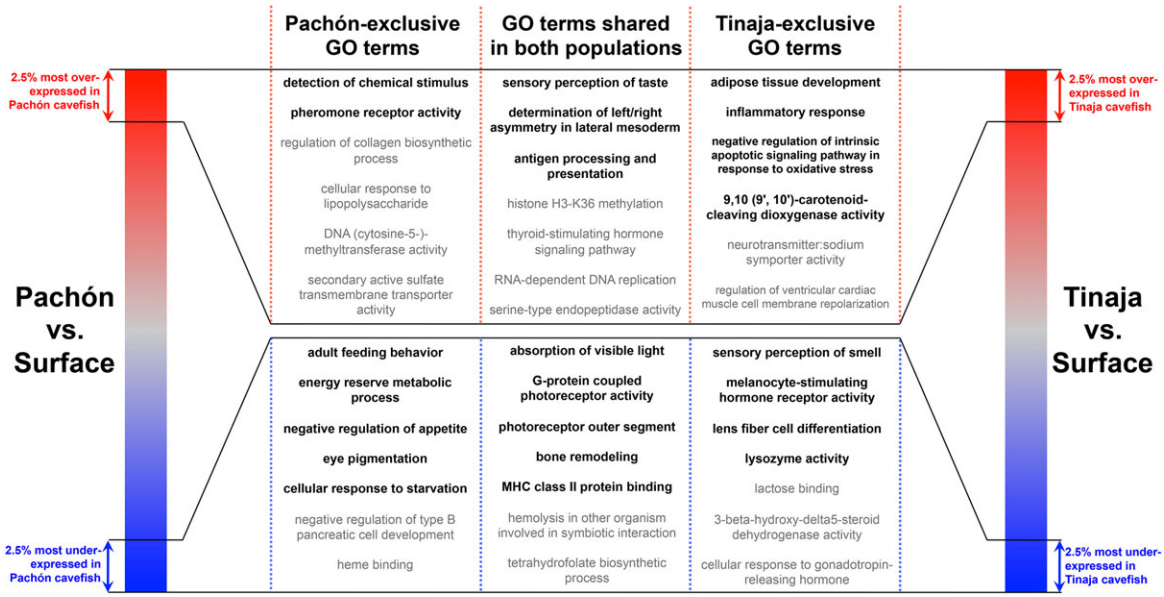


**Figure 2.** GO enrichment studies reveal shared and unique gene functions in Pachón and Tinaja lineages. RNA-seq studies identified dramatic gene expression differences in Pachón and Tinaja cavefish relative to the surface form. We described the biological functions and processes associated with the most differentially expressed genes in our data set. Many of the same gene ontology terms were enriched in the top 2.5% of differentially overexpressed (red) or underexpressed (blue) genes in Pachón cavefish (left side) and Tinaja (right side). However, this gene ontology enrichment study also revealed a number of terms unique to Pachón and Tinaja cavefish lineages (left and right sides, respectively). [Color figure can be viewed at wileyonlinelibrary.com]

ulus" and "pheromone receptor activity." Interestingly, *Tas21rl*, a gene encoding a taste receptor, was upregulated in both caves. However, the gene *V1r1l*, which encodes a putative pheromone receptor, contributed to this enrichment only in Pachón cavefish. Conversely, upregulation of another gene associated with tastant detection, *Tas2r202*, was uniquely detected in Tinaja cave. This may indicate that selection for cave-associated phenotypes occurs at the level of gene function, which may or may not include the orthologous gene in different cavefish lineages.

We discovered several unexpected GO terms enriched in both cave populations. For instance, in the underexpressed gene sets, we identified "negative regulation of type B pancreatic cell development," "heme binding," "tetrahydrofolate biosynthetic process," and "lactose binding." In the overexpressed gene sets, we observed "DNA (cytosine-5-)-methyltransferase activity," "histone H3-K36 methylation," "thyroid-stimulating hormone signaling pathway," and "neurotransmitter: sodium symporter activity." Future studies will clarify how these unpredicted ontology terms are associated with adaptation to the cave environment.

### Convergence at the Level of Individual Genes in two Distinct Cavefish Lineages

We identified shared genes in both cave populations demonstrating the highest fold-change differences (≥10-fold; Methods section). Several of the identified genes impact on visual system development, maintenance, and function. Interestingly, in both cave populations, an eye begins to form, but begins to degenerate at ~24 hpf (Jeffery, 2009b). Our cross-developmental results reflect this degeneration. For instance, early on (~10 hpf) only one eye-related gene, *Bcmo1*, demonstrates substantial reduced expression. However, beginning at 24 hpf additional vision-related genes demonstrate substantial reduction in expression (Table 1; Supplementary Table S6), including *Irbp*. By 36 hpf, *Lim2 and Mipa* similarly show reduced expression. By the last developmental timepoint (72 hpf), the genes *Crx*, *Hsp5*, *Vsx1*, *Nrl*, *and Impg2* were reduced in expression in both cave populations. Many of these genes (*Lim2*, *Mipa*, and *Crx*) have been previously characterized in the context of aberrant eye development/size in cavefish (Jeffery and Strickler, 2003; Strickler and Jeffery, 2009; Pottin et al., 2011; Gross et al., 2013; O'Quin et al., 2013; McGaugh et al., 2014). However, this study is the first to demonstrate reduced expression of these genes in two geologically distinct eyeless cavefish populations. Moreover, our dynamic expression profiles revealed that as the eye is lost over the course of development, the numbers of genes with altered expression mirrors this morphological degeneration.

Two of the genes identified, *Nrl* and *Impg2*, may play key roles in *Astyanax* eye loss. For instance, the gene *Nrl*, involved

Table 1. Genes demonstrating convergent and divergent patterns of expression in both Pachón and Tinaja cavefish compared to surface-dwelling fish.

| Expression pattern | Gene | Transcript ID | Physiological function(s)[a] | Pachón cavefish (fold change)[b] | Tinaja cavefish (fold change)[b] |
|---|---|---|---|---|---|
| **10 hpf** | | | | | |
| Convergent reduced | *Fads2* | ENSAMXT00000016443 | Fatty acid biosynthetic process | 20.832 down[c] | 40.975 down[c] |
| Convergent reduced | *Bcmo1* | ENSAMXT00000010290 | **Eye photoreceptor; hindbrain** | 21.458 down[c] | 10.005 down[c] |
| Convergent increased | *Tas2r1l* | ENSAMXT00000006165 | **Sensory perception of taste** | 70.497 up[c] | 234.314 up[c] |
| Convergent increased | *Bco2a* | ENSAMXT00000003245 | **Pigmentation** | 14.021 up[c] | 17.053 up[c] |
| Divergent—Pachón reduced | *Shisa6* | ENSAMXT00000016152 | **Eye; retina** | 78.748 down[c] | 2.057 up |
| Divergent—Pachón reduced | *Btk* | ENSAMXT00000002400 | **Eye;** whole organism | 92.641 down[d] | 1.551 down |
| Divergent—Tinaja reduced | *Mchr1a* | ENSAMXT00000009888 | **Pigmentation** | 1.713 up | 23.202 down[c] |
| Divergent—Tinaja reduced | *Mhcf10la* | ENSAMXT00000012479 | **Immune response** | 4.165 up | 118.172 down[c] |
| Divergent—Pachón increased | *Trpa1a* | ENSAMXT00000008706 | **Sensory perception** | 115.042 up[d] | 3.185 down |
| Divergent—Pachón increased | *Dfnb59* | ENSAMXT00000004928 | **Auditory system; inner ear** | 37.118 up[c] | No change |
| Divergent—Tinaja increased | *Bco2l* | ENSAMXT00000005225 | **Pigmentation** | No change | 111.277 up[c] |
| Divergent—Tinaja increased | *Adcyap1a* | ENSAMXT00000007454 | **Eye development;** brain development | 4.948 up | 18.826 up[d] |
| **24 hpf** | | | | | |
| Convergent reduced | *Soul4* | ENSAMXT00000004688 | **Digestion** | 367.405 down[c] | 3192.621 down[c] |
| Convergent reduced | *Oca2* | ENSAMXT00000013137 | **Pigmentation** | 16.356 down[d] | 11.361 down[d] |
| Convergent increased | *Topl* | ENSAMXT00000019646 | Oxidative stress; heme binding | 89.712 up[d] | 50.468 up[d] |
| Convergent increased | *Trim35* | ENSAMXT00000002908 | Zinc ion binding | 624.919 up[c] | 184.620 up[c] |
| Divergent—Pachón reduced | *Vsx2* | ENSAMXT00000011986 | **Eye; retina** | 17.223 down[c] | 6.633 down |
| Divergent—Pachón reduced | *C1galt1* | ENSAMXT00000016160 | Transferase activity | 528.520 down[c] | 1.710 up |
| Divergent—Tinaja reduced | *Pmchl* | ENSAMXT00000026184 | **Pigmentation** | 2.445 down | 492.004 down[c] |
| Divergent—Tinaja reduced | *Hsf4* | ENSAMXT00000021068 | **Lens morphogenesis in camera-type eye** | 3.417 down | 60.965 down[c] |
| Divergent—Pachón increased | *Dlg4b* | ENSAMXT00000020555 | **Retina; olfactory bulb;** midbrain | 245.106 up[c] | No change |
| Divergent—Pachón increased | *Crygm4* | ENSAMXT00000008090 | **Eye; lens constituent** | 177.556 up[c] | No change |

(*Continued*)

Table 1. Continued

| Expression pattern | Gene | Transcript ID | Physiological function(s)[a] | Pachón cavefish (fold change)[b] | Tinaja cavefish (fold change)[b] |
|---|---|---|---|---|---|
| Divergent—Tinaja increased | *Hla-F10al* | ENSAMXT00000003617 | Immune response | 2.726 up | 88.106 up[d] |
| Divergent—Tinaja increased | *H2-IEbl* | ENSAMXT00000005358 | Immune response; MHC class II protein | No change | 700.042 up[c] |
| **36 hpf** | | | | | |
| Convergent reduced | *Mipa* | ENSAMXT00000004665 | Lens development | 29.444 down[c] | 2691.257 down[c] |
| Convergent reduced | *Lim2* | ENSAMXT00000004471 | Lens constituent | 21.287 down[c] | 25.195 down[c] |
| Convergent increased | *RNF213* | ENSAMXT00000006372 | Metabolic process, protein ubiquitination | 59.725 up[c] | 64.117 up[c] |
| Convergent increased | *Plb1* | ENSAMXT00000025263 | Lipid metabolic process | 179.225 up[c] | 76.688 up[c] |
| Divergent—Pachón reduced | *Six7* | ENSAMXT00000016345 | Embryonic camera-type eye | 59.027 down[c] | 4.105 down |
| Divergent—Pachón reduced | *Itln2* | ENSAMXT00000003593 | Defense response | 470.848 down[c] | 1.063 up |
| Divergent—Tinaja reduced | *Chordc1a* | ENSAMXT00000003933 | Hsp90 protein binding | 4.997 down | 3610.523 down[c] |
| Divergent—Tinaja reduced | *Or128-10* | ENSAMXT00000026303 | Olfaction | 1.295 up | 183.637 down[c] |
| Divergent—Pachón increased | *Phf20a* | ENSAMXT00000002218 | Zinc ion binding | 234.814 up[c] | 5.453 up |
| Divergent—Pachón increased | *Gxylt1b* | ENSAMXT00000017058 | Transferase activity, transfer glycosyl | 151.277 up[c] | No change |
| Divergent—Tinaja increased | *Endo1* | ENSAMXT00000004210 | Nucleic acid binding; hydrolase activity | 4.124 up | 466.036 up[c] |
| Divergent—Tinaja increased | *Or104-2* | ENSAMXT00000021297 | Odorant receptor | No change | 91.607 up[c] |
| **72 hpf** | | | | | |
| Convergent reduced | *Vsx1* | ENSAMXT00000011754 | Visual system | 32.800 down[c] | 15.161 down[c] |
| Convergent reduced | *Crx* | ENSAMXT00000001606 | Visual perception | 31.387 down[c] | 13.068 down[c] |
| Convergent increased | *Or115-15* | ENSAMXT00000025780 | Sensory perception of smell | 204.065 up[c] | 323.993 up[c] |
| Convergent increased | *Mr1* | ENSAMXT00000009606 | Immune response; antigen processing | 68.836 up[d] | 62.073 up[d] |
| Divergent—Pachón reduced | *Agrp* | ENSAMXT00000005977 | Pigmentation | 382.851 down[c] | 1.038 up |
| Divergent—Pachón reduced | *Impg1a* | ENSAMXT00000010962 | Photoreceptor | 100.072 down[c] | 3.291 down |
| Divergent—Tinaja reduced | *Crygn2* | ENSAMXT00000018569 | Lens constituent | 2.900 up | 1791.267 down[c] |
| Divergent—Tinaja reduced | *Irx7* | ENSAMXT00000000343 | Retina morphogenesis | 1.526 down | 17.011 down[c] |

(*Continued*)

Table 1. Continued

| Expression pattern | Gene | Transcript ID | Physiological function(s)[a] | Pachón cavefish (fold change)[b] | Tinaja cavefish (fold change)[b] |
|---|---|---|---|---|---|
| Divergent—Pachón increased | *Sb:cb1081* | ENSAMXT00000018849 | **Eye; lens constituent** | 880.522 up[c] | 2.117 down |
| Divergent—Pachón increased | *Tas2r1l* | ENSAMXT00000006165 | **Sensory perception of taste** | 38.398 up[c] | 5.496 up |
| Divergent—Tinaja increased | *Olfm4* | ENSAMXT00000014744 | **Olfaction** | 2.633 down | 164.740 up[c] |
| Divergent—Tinaja increased | *Gh1* | ENSAMXT00000015091 | **Adipose tissue development** | 5.171 down | 143.272 up[c] |

[a]Physiological functions are determined by a combination of gene ontology and known literature. Functions in bold may be associated with troglomorphic traits.
[b]Genes are under- or overexpressed 10-fold or greater in both Pachón and Tinaja cavefish compared to surface. Blue indicates underexpressed, and red indicates overexpression.
[c]$P$-value $< 0.05$.
[d]$P$-value $< 0.10$. Statistics calculated using Student's $t$-test with FDR, as the difference of normalized reads between Pachón or Tinaja to surface fish.

in opsin expression, is also downregulated the Chinese cavefish species *Sinocyclocheilus* (Meng et al., 2013). Similarly, the retinal gene *Impg2* is inactivated (a pseudogene with two splice acceptor mutations and a frameshift deletion) in the subterranean-dwelling Cape golden mole, *Chrysochloris asiatica* (Emerling and Springer, 2014). Further, *Impg2* variants are associated with autosomal recessive forms of retinitis pigmentosa in humans (Bandah-Rozenfeld et al., 2010). Thus, many of the same genes participate in normative and disease-associated eye loss across deep vertebrate lineages of subterranean animals and humans.

Two genes involved in pigmentation were convergently underexpressed, including *Oca2* at 24 hpf and *Mitfa* at 36 hpf. The reduced-expression of *Oca2* was unsurprising as it was previously identified as the locus governing albinism in Pachón, Molino, and Japonés cave populations (Protas et al., 2006). Interestingly, Pachón cavefish harbor both destructive coding sequence alterations as well as reduced expression of *Oca2* (16.356 down); while Tinaja cavefish demonstrate solely reduced expression (11.361 down), but an unaltered *Oca2* coding sequence. This result is consistent with prior research directly demonstrating reduction of *Oca2* transcriptional abundance using in situ hybridization (Bilandzia et al., 2013).

The gene *Mitfa* shows reduced expression in both cave populations. This is a highly conserved transcription factor involved in the melanocortin signaling pathway, and reduced expression of *Mitfa* causes a reduction in expression of several downstream pigmentation genes (Shibara et al., 2001; Levy et al., 2006). We also observed convergent, reduced expression in genes for which a functional role in cave evolution is unknown. For instance, the gene *Soul4* (predicted to function in heme binding) demonstrates significantly lower expression across development in Pachón and Tinaja. Future studies will clarify the precise role of *Soul4* in cave adaptation.

Cave animals also evolve constructive traits that facilitate life in complete darkness. Constructive characters include expansion of nonvisual sensory systems such as enhanced lateral line, increased numbers of taste buds, heightened odorant sensitivity, increased fat reserves, and resistance to starvation (Jeffery, 2009a). Our analyses revealed increased expression of a gene encoding a taste receptor (*Tas2r1l*) in both Pachón and Tinaja cavefish populations. Studies in other systems such as humans, *Drosophila*, and zebrafish suggest that *Tas2r* genes are related to bitter taste receptors, and therefore abundance of this receptor type may enable cavefish to detect aversive tastants and diverse organic compounds at a very low threshold (Oike et al., 2007; Aihara et al., 2008). Similarly, the odorant receptor gene, *Or115-15* (involved in odorant perception), was overexpressed in both cavefish lineages at 72 hpf. The heterologous expression of this receptor protein in a baculovirus/Sf9 cell system showed that Or115 receptor types responded to the potent odorant pyrazine (Breer et al., '98; Lévai et al., 2006). These gene expression changes are consistent with a recent study demonstrating that embryonic cavefish have larger olfactory placodes and higher sensitivity to amino acids compared to surface fish (Hinaux et al., 2016). Thus, selection for increased expression of these odorant receptors may enable cavefish to detect low levels of nutritive substrate (or aversive chemicals) in the complete darkness of the cave.

Increased deposition of yellow-orange carotenoid pigments has been previously documented in Pachón (Culver and Wilkens,

2000) and observed at a modest level in Tinaja cavefish relative to surface fish (pers. obs.; Fig. 1). Interestingly, we detected convergent patterns of increased expression in *Bco2a* across embryonic development. This gene encodes an enzyme (beta-carotene dioxygenase), which asymmetrically cleaves carotenoids to render a colorless compound. Numerous examples of "yellow" phenotypes are observed in cow (Tian et al., 2012), sheep (Våge and Bowman, 2010), chicken (Eriksson et al., 2008), and rabbits (Strychalski et al., 2016) as a consequence of alterations affecting *Bco2*. The fact that Pachón cavefish demonstrate a yellowish coloration, but also express abundant transcripts of *Bco2* is curious. Future studies will clarify if this upregulation is persistent in all tissues (or, perhaps downregulated in the skin). Alternatively, despite upregulation at the level of the transcript, this enzyme may be rapidly degraded, leading to the yellowish appearance in Pachón.

### Unique Gene Expression Patterns are Observed in Each Cavefish Population

The gross appearance of *Astyanax* cavefish drawn from different caves are highly similar (Fig. 1). However, cavefish lineages differ substantially in terms of their evolutionary histories (Gross, 2012), identity of the genes mediating eye loss (Borowsky, 2008) and melanophore pigmentation (Gross et al., 2009). Phenotypic and physiological differences are frequently accompanied by genetic changes including alterations in gene expression. Pachón and Tinaja cave populations demonstrated divergent expression patterns in numerous vision-related genes. Across the four stages assayed, several genes showed reduced expression unique to Pachón cavefish, including *Btk* and *Shisa6* at 10 hpf, *Vsx2* at 24 hpf, *Irbp* and *Six7* at 36 hpf, and *Opn4.1*, *Rgrb* and *Impg1a* at 72 hpf (Table 1; Supplementary Table S6).

Our analyses also revealed new candidate gene expression profiles that provide a clue to the genetic basis for eye loss in cavefish. For example, *Six7* demonstrated uniquely reduced expression in Pachón cavefish (59.027 down at 36 hpf), but not Tinaja cavefish. *Six7* is expressed during embryonic retinal morphogenesis in camera-type eyes and rod cells of zebrafish (Saade et al., 2013). The loss of both *Six7* and *Six3b* results in microphthalmia or anophthalmia in zebrafish mutants (Inbal et al., 2007). Additional functional analysis will help discern the role of *Six7* in the naturally occurring anophthalmia of Pachón cavefish.

Several lens-related genes demonstrated reduced expression in cavefish, including members of the *crystallin* family (e.g., *Cryba1l*). These expression changes may not directly cause visual system loss in cavefish, but reflect a consequence of reduced lens size due to apoptosis at ~36 hpf (Hinaux et al., 2015). Interestingly, Tinaja cavefish showed reduced expression in 11 *different* eye-related genes, varying by developmental stage. These included *Opn4b*, *Hsf4*, and *Opn1mw4* at 24 hpf, and *Elavl1*, *Crygn2*, *Irx7*, and *Ndr2* at 72 hpf (Table 1; Supplementary Table S6). *Crygn2* has been implicated in other Pachón eye loss studies (Gross et al., 2013; O'Quin et al., 2013). Our expression analyses indicate that Pachón and Tinaja harbor a mix of both shared and distinct eye genes, demonstrating differential expression across development. This supports the notion that Pachón and Tinaja cavefish are more closely related than other cavefish lineages owing to the lower percentage of individuals demonstrating complementation of the visual system (Borowsky, 2008). Thus, assuming early gene expression patterns predict the absence of a visual system by juvenilehood, we would expect a mixture of both shared and distinct genes mediating this eye loss phenotype.

Body pigmentation loss is present widely across the *Astyanax* cavefish landscape. The genetic basis for two degenerative pigmentation traits are *Oca2* (albinism) in Pachón, Molino, and Japonés caves; and *Mc1r* (*brown*) in Pachón and Yerbaníz/Japonés subterranean lineages (Protas et al., 2006; Gross et al., 2009). The genes causing reduced pigmentation in other cave populations (e.g., Tinaja) remain largely unknown. In Pachón cavefish, we discovered reduced expression of five pigmentation genes, including *Smtlb* and *Pomca* at 36 hpf, and *Mc4r* (Aspiras et al., 2015), *Agrp*, and *Tyr* at 72 hpf (Table 1; Supplementary Table S6). Although Pachón cavefish are albino owing to a large exon deletion in *Oca2*, our findings show that many other genes such as *Tyr* (12.772 down) involved in the melanogenesis pathway are also affected (Garcia-Borron et al., 2005; Protas et al., 2006). This may suggest that the accumulation of mutations in multiple genes contributing to pigmentation in Pachón cavefish occurs as a consequence of neutral mutation (Protas et al., 2007).

Interestingly, Tinaja cave-dwelling fish show reduced expression in *distinct* pigmentation genes across development, including *Mch1ra* at 10 hpf, *Mlpha* and *Pmchl* at 24 hpf, *Mc1r* at 36 hpf, and *Mchr2* at 72 hpf (Table 1; Supplementary Table S6). Similar to *Oca2*, the gene *Mc1r* (58.100 down) harbors both coding sequence mutations and reduced expression in Pachón cavefish (Gross et al., 2009; Stahl and Gross, 2001). Another candidate gene, *Mlpha* (102.456 down), plays a key role in melanocyte differentiation and melanosome localization. This gene is linked to aggregated melanosomes/disrupted pigment granule dispersion in zebrafish (Thisse and Thisse, 2004), dilute coat color in cats (Ishida et al., 2006), and Griscelli syndrome type 3 (light hair and skin color) in humans (Ménasché et al., 2005). Thus, *Mlpha* may play a role in cave-associated pigmentation loss analogous to other distantly related vertebrate species. Finally, we characterized additional uniquely impacted genes associated with life in total darkness (Table 1; Supplementary Table S6).

Pachón and Tinaja cavefish also demonstrated uniquely divergent patterns of gene overexpression. Pachón cavefish harbor increased gene expression associated with nonvisual sensory traits, such as taste: *Vn1r1* at 10 hpf and *Tas2r1l* at 72 hpf; mechanical stimulus/neuromast development: *Trpa1a* at 10 hpf; olfaction: *Dlg4b* at 24 hpf; and auditory sensation: *Dfnb59* at 10

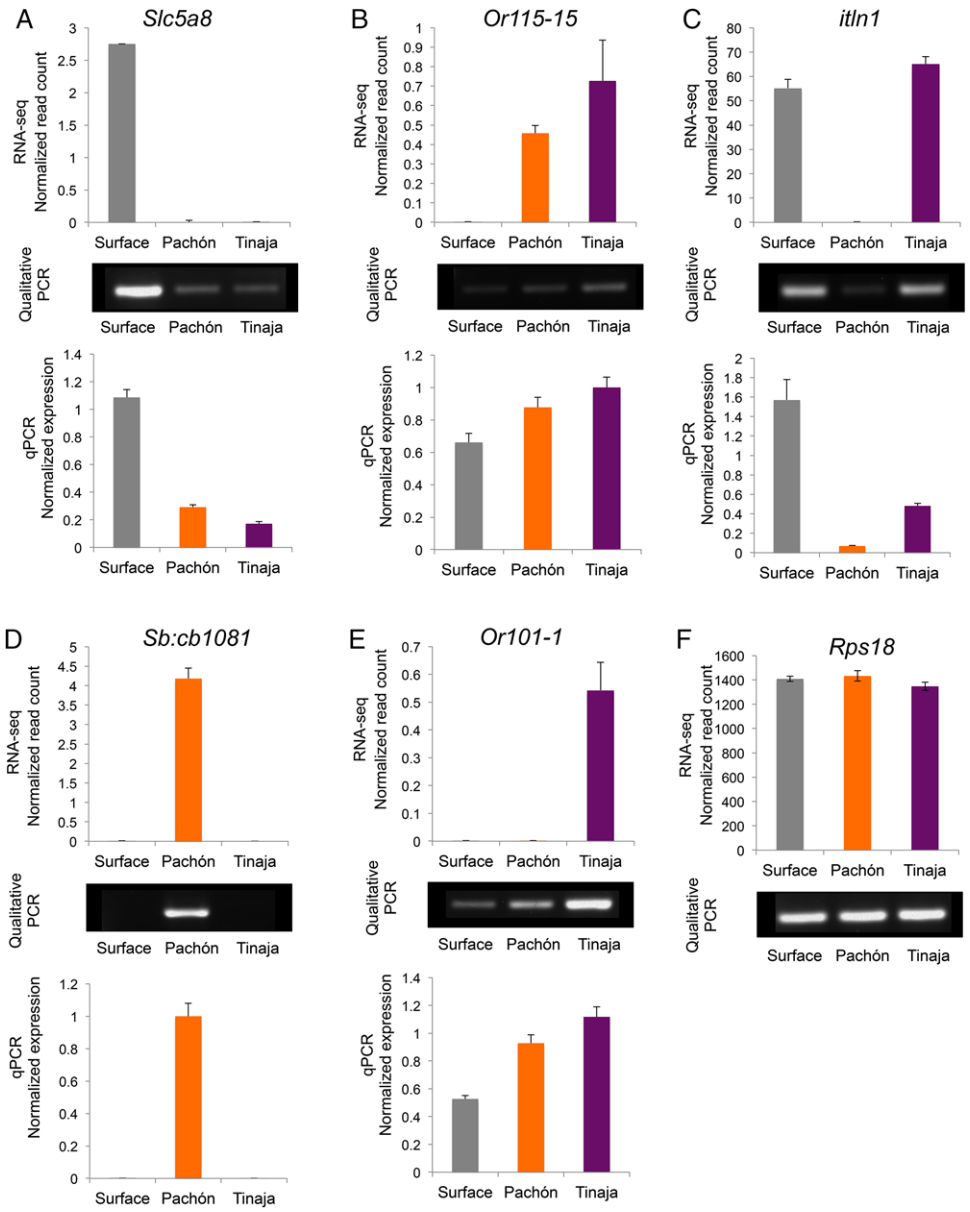


**Figure 3.** Qualitative and quantitative PCR analyses validate a subset of genes representing diverse expression profiles at 72 hpf. To confirm diverse expression profiles observed in our RNA-seq comparison, we validated the normalized expression pattern (top graphs) for a subset of experimental genes at 72 hpf using both qualitative (gel images) and qPCR analyses (bottom graphs). Two genes *Slc5a8* (A) and *Or115-15* (B) demonstrated convergent expression in Pachón and Tinaja. The gene *itln1* (C) showed higher expression in surface fish and Tinaja cavefish, but reduced expression in Pachón cavefish. Conversely, the gene *Sb:cb1081* (D) was expressed at high levels in Pachón cavefish, but reduced in expression in surface and Tinaja cavefish. Finally, the gene *Or101-1* (E) demonstrated an expression profile in which the highest level was found in Tinaja cavefish, the lowest level was observed in surface fish, and an intermediate level of expression was found in Pachón cavefish. For all experiments, we utilized the reference gene *Rps18* as a control gene demonstrating the same level of expression in all groups (F). Each "representative" gene evaluated in this experiment demonstrated significant expression differences across each of the three morphotypes. [Color figure can be viewed at wileyonlinelibrary.com]

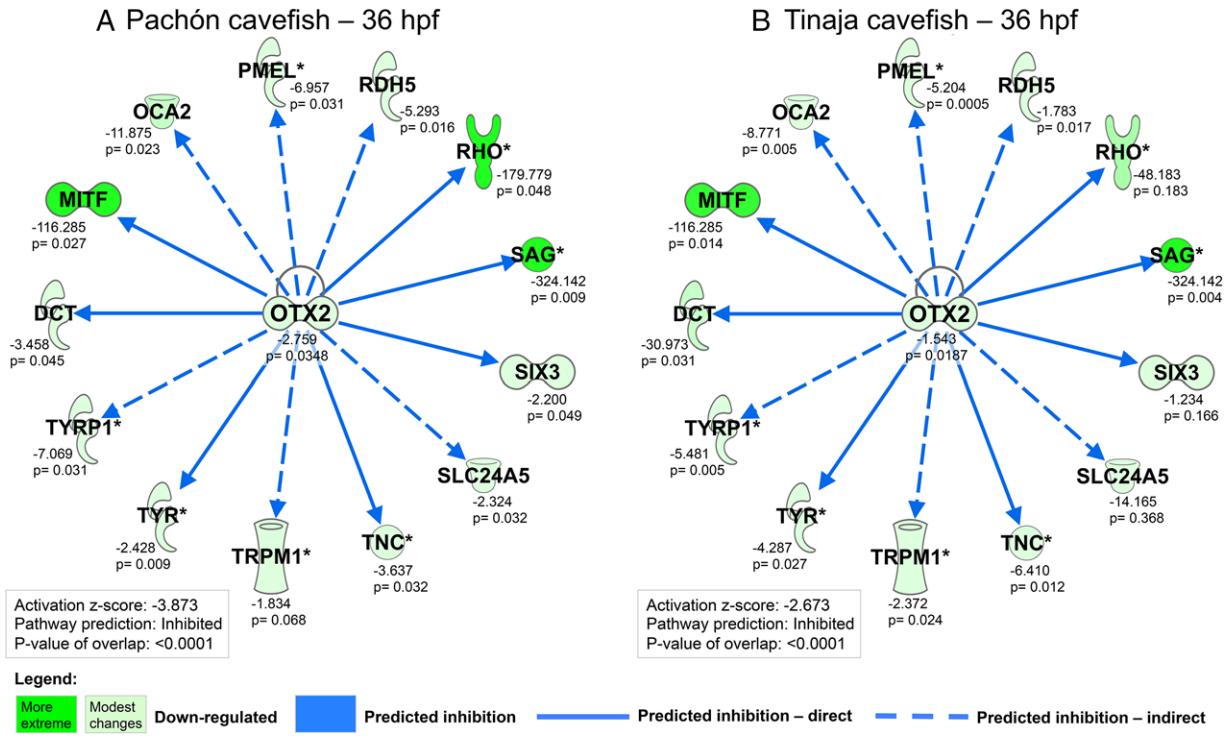


**Figure 4.** Pathway analysis reveals *Otx2* is a crucial upstream regulator governing regressive vision and pigmentation loss in different cave populations. We employed ingenuity pathway analysis (IPA) to identify upstream gene regulators that may explain the observed expression patterns across our experimental data set. Using this analysis, we detected *Otx2* as a potential upstream regulator inhibited in both Pachón (A) and Tinaja (B) cavefish at 36 hpf. [Color figure can be viewed at wileyonlinelibrary.com]

hpf (Table 1; Supplementary Table S6). Pachón also overexpress the gene *Trpa1a* (115.042 up), a known regulators of chemosensation in zebrafish (Prober et al., 2008), thermal nociception in *Drosophila* (Neely et al., 2011), and *episodic pain syndrome familial 1* in rats and humans (Kremeyer et al., 2010; Chen et al., 2011). The gene *Dfnb59* (37.118 up), also uniquely overexpressed in Pachón, and when inhibited in humans and mice results in auditory loss through inner ear hair cell dysfunction (Delmaghani et al., 2006; Ebermann et al., 2007). Tinaja cavefish also demonstrate heightened extravisual sensation; however, different genes likely underlie these constructive adaptations (Table 1; Supplementary Table S6). For instance, overexpression of several olfaction genes, including *Or104-2* at 36 hpf and *Or101-1*, *Olfm4*, *Or132-5*, and *Or115-15* at 72 hpf, and taste-associated genes, such as *Tas2r202* and *Tas1r3* at 72 hpf, was found exclusively in the Tinaja data set. Finally, genes related to adipose tissue storage, response to starvation, and visual perception showed profiles of increased expression within each cave (Table 1; Supplementary Table S6). We confirmed several of these profiles for a subset of genes at 72 hpf using qualitative and quantitative PCR (Fig. 3).

### Pathway Analysis Reveals Otx2 and Mitf as Crucial Upstream Regulators Selected in Two Ancient Cavefish Lineages

To determine if key upstream regulators may have been selected in both cave lineages, we utilized IPA to evaluate global expression profiles. We mapped extensive annotation information to a total of 17,897 of 23,719 *Astyanax* genes in our data set. We used the "IPA regulator" tool to reveal upstream transcriptional regulators explaining global patterns of expression change in our data set. We concentrated our efforts on identifying regulators affecting eye degeneration and reduced pigmentation.

Putative regulators were identified based upon expression patterns in both cave lineages, relative to surface fish, at 36 hpf. At this developmental time point, melanin begins to appear in surface fish but remains absent in cave. In addition, by 36 hpf, cavefish eyes have begun to degenerate (Jeffery, 2005, 2009b). Thus, an altered upstream regulator at this developmental stage would impact both pigmentation and vision in cavefish. In Pachón cavefish, our analysis identified 40 prospective upstream regulators as "activated" (activation z-score > 2.0) and 53 potential "inhibited" regulators (activation *z*-score < −2.0). Similarly, we

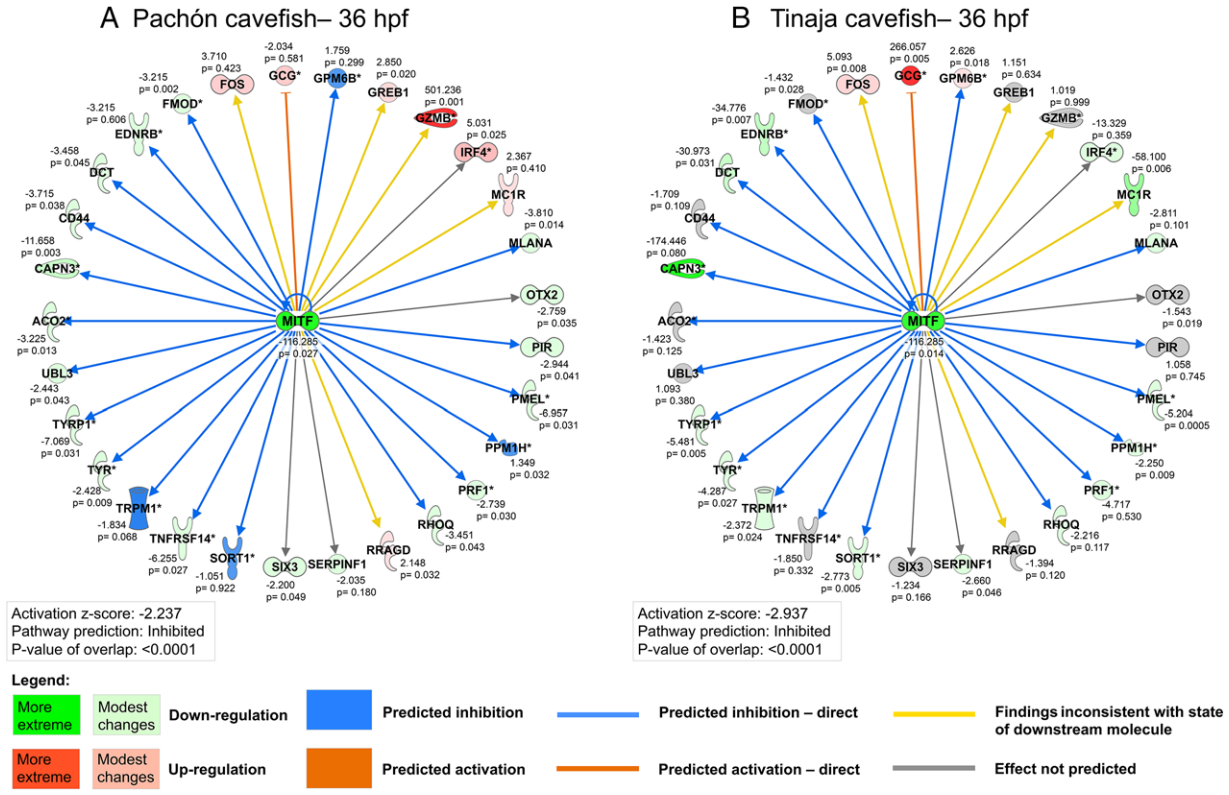


Figure 5. Pathway analysis implicates *Mitf* as a potential upstream regulator in Pachón and Tinaja cavefish at 36 hpf. We used ingenuity pathway analysis (IPA) to nominate potential upstream genetic regulators that could explain expression changes in downstream target genes. In our parallel studies, we detected *Mitf*–which encodes a critical transcription factor for numerous pigmentation-related processes– as a potential regulator that is inhibited in both Pachón (A) and Tinaja (B) cavefish lineages at 36 hpf. [Color figure can be viewed at wileyonlinelibrary.com]

identified 86 "activated" and 56 "inhibited" regulators in Tinaja cavefish.

The same gene was the top predicted upstream "inhibited" regulator in both cave populations. The gene *Otx2* was identified in both Pachón cavefish (fold change = −2.759, predicted activation state = inhibited, *z*-score = −3.873, *P*-value < 0.0001; Fig. 4A) and Tinaja cavefish (fold change = −1.543, predicted activation state = inhibited, *z*-score = −2.673, *P*-value < 0.0001; Fig. 4B). *Otx2* is a well-characterized transcriptional regulator that, when altered in humans and zebrafish, results in retinal dystrophy and microphthalmia (Wyatt et al., 2008; Chassaing et al., 2012; Vincent et al., 2014). A whole-mount in situ hybridization series (10–48 hpf) in *A. mexicanus* revealed an overall decrease in *Otx2* gene expression in Pachón cavefish compared to surface fish. Further, in situ sections of both morphs at 48 hpf revealed significantly reduced *Otx2* expression in the cavefish lens (McGaugh et al., 2014). Downstream targets of *Otx2* include other eye-related genes and several genes with known roles in melanization, including *Oca2* (Fig. 4A and B).

We further screened our results to identify inhibited targets relevant to pigmentation. We uncovered *Mitf*, a transcription factor governing diverse pigment-related processes, in both Pachón (fold change = −116.285, predicted activation state = inhibited, *z*-score = 2.237, *P*-value < 0.0001; Fig. 5A) and Tinaja (fold change = −116.285, predicted activation state = inhibited, *z*-score = −2.937, *P*-value < 0.0001; Fig. 5B) including several downstream targets (e.g., *Mc1r*). Interestingly, the recently published draft genome for cavefish predicts a severe truncation in the coding structure of *Mitf*. At present, this truncation has not been confirmed, and therefore it may represent an artifact of genome assembly or annotation. Irrespective, it will be interesting to determine if the observed downregulation of numerous downstream genes is attributable to this putative genetic lesion in *Mitf*, and if the same genetic lesion is present in other cave populations.

Overall, these results suggest that certain key genes and pathways are repeatedly altered, albeit at different levels, in independent cavefish lineages. Further, the pleiotropic consequences

of inhibited upstream factors could contribute to the numerous cave-adapted traits observed in *Astyanax* cave-dwelling fish.

## CONCLUSIONS

This study assessed that global gene expression changes accompanying cave isolation for two geographically distinct cavefish populations. From these comparisons, we discovered that Pachón and Tinaja cavefish evolved dramatic changes in gene expression in several of the same genes, perhaps as a result of gene flow or selective pressure. For certain traits, this may reflect a common genetic basis for certain shared morphologies between *Astyanax* cavefish populations, despite geographic and phylogenetic differences. However, our analyses also revealed many expression differences exclusive to each cavefish population, suggesting subtle differences in subterranean habitats and phylogenetic histories lead to cave-specific gene expression differences. This study further indicates that these remarkable animals manifest a spectrum of cave-adapted traits through a combination of both convergent and divergent genetic mechanisms, and identifies numerous genes that contribute to extreme trait evolution in natural populations. Although this study highlights an array of intriguing genes with prospective roles in cave evolution based on the convergent and divergent expression profiles in Pachón and Tinaja cavefish populations, future functional studies will be crucial for clarifying their precise roles in cave-dwelling *Astyanax*. Finally, although this report characterizes a subset of genes with polarized differences in expression, it is likely many additional genes with modest expression changes likely contribute to the diverse troglomorphic traits in *Astyanax* cave lineages.

## ACKNOWLEDGMENTS

The authors wish to thank Brian M. Carlson and Amanda K. Powers of the Gross lab for assistance with embryo collection and helpful discussions. We also thank Dr. Richard Borowsky (New York University) for generously providing the adults used for breeding in this study. In addition, we are grateful for the guidance of Dr. Suzanne McGaugh (University of Minnesota) with the pathway analysis and for the resources of the University of Minnesota Supercomputing Institute. The authors declare no conflict of interest with this manuscript.

### Conflict of interest

None.

## LITERATURE CITED

Abou-Rayyah Y, Collin JR, Robinson D. 2008. Novel heterozygous *OTX2* mutations and whole gene deletions in anophthalmia, microphthalmia and coloboma. Hum Mutat 29:E278–E283.

Aihara Y, Yasuoka A, Iwamoto S, et al. 2008. Construction of a taste-blind medaka fish and quantitative assay of its preference–aversion behavior. Genes Brain Behav 7:924–932.

Aspiras AC, Rohner N, Martineau B, Borowsky RL, Tabin CJ. 2015. Melanocortin 4 receptor mutations contribute to the adaptation of cavefish to nutrient-poor conditions. Proc Natl Acad Sci USA 112:9668–9673.

Bandah-Rozenfeld D, Collin R, Banin E. 2010. Mutations in *IMPG2*, encoding interphotoreceptor matrix proteoglycan 2, cause autosomal-recessive retinitis pigmentosa. Am J Hum Genet 87:199–208.

Benjamini Y, Hochberg Y. 2000. On the adaptive control of the false discovery rate in multiple testing with independent statistics. J Educ Behav Stat 25:60–83.

Bilandžija H, Ma L, Parkhurst A, Jeffery WR. 2013. A potential benefit of albinism in *Astyanax* cavefish: Downregulation of the *oca2* gene increases tyrosine and catecholamine levels as an alternative to melanin synthesis. PLoS One 8:e80823.

Borowsky R. 2008. Restoring sight in blind cavefish. Curr Biol 18:R23–R24.

Bradic M, Beerli P, García-de León FJ, Esquivel-Bobadilla S, Borowsky RL. 2012. Gene flow and population structure in the Mexican blind cavefish complex (*Astyanax mexicanus*). BMC Evol Biol 12:9.

Breer H, Krieger J, Meinken C, Kiefer H, Strotmann J. 1998. Expression and functional analysis of olfactory receptors. Ann NY Acad Sci 855:175–181.

Chassaing N, Sorrentino S, Davis EE, et al. 2012. *OTX2* mutations contribute to the otocephaly-dysgnathia complex. J Med Genet 49:373–379.

Chen J, Joshi SK, DiDomenico S, et al. 2011. Selective blockade of TRPA1 channel attenuates pathological pain without altering noxious cold sensation or body temperature regulation. Pain 152:1165–1172.

Culver DC, Wilkens H. 2000. Critical review of the relevant theories of the evolution of subterranean animals. In: Wilkens H, Culver DC, Humphreys WF, editors. Ecosystems of the World v. 30. Subterranean Ecosystems. Amsterdam: Elsevier. p 381–398.

Delmaghani S, del Castillo FJ, Michel V, et al. 2006. Mutations in the gene encoding pejvakin, a newly identified protein of the afferent auditory pathway, cause DFNB59 auditory neuropathy. Nat Genet 38:770–778.

Ebermann I, Walger M, Scholl HP, et al. 2007. Truncating mutation of the *DFNB59* gene causes cochlear hearing impairment and central vestibular dysfunction. Hum Mutat 28:571–577.

Emerling CA, Springer MS. 2014. Eyes underground: regression of visual protein networks in subterranean mammals. Mol Phylogenet Evol 78:260–270.

Eriksson J, Larson G, Gunnarsson U, et al. 2008. Identification of the *yellow skin* gene reveals a hybrid origin of the domestic chicken. PLoS Genet 4:e1000010.

Garcia-Borron JC, Sanchez-Laorden BL, Jimenez-Cervantes C. 2005. Melanocortin-1 receptor structure and functional regulation. Pigment Cell Res 18:393–410.

Gross JB. 2012. The complex origin of *Astyanax* cavefish. BMC Evol Biol 12:105.

Gross JB, Wilkens H. 2013. Albinism in phylogenetically and geographically distinct populations of *Astyanax* cavefish arises through the same loss-of-function *Oca2* allele. Heredity 111:122–130.

Gross JB, Borowsky R, Tabin CJ. 2009. A novel role for *Mc1r* in the parallel evolution of depigmentation in independent populations of the cavefish *Astyanax mexicanus*. PLoS Genet 5:e1000326–e1000394.

Gross JB, Furterer A, Carlson BM, Stahl BA. 2013. An integrated transcriptome-wide analysis of cave and surface dwelling *Astyanax mexicanus*. PLoS ONE 8:e55659.

Gross JB, Krutzler A, Carlson B. 2014. Complex craniofacial changes in blind cave-dwelling fish are mediated by genetically symmetric and asymmetric loci. Genetics 196:1303–1319.

Guaiquil VH, Pan Z, Karagianni N. 2014. *VEGF-B* selectively regenerates injured peripheral neurons and restores sensory and trophic functions. Proc Natl Acad Sci USA 111:17272–17277.

Hinaux H, Pottin K, Chalhoub H, et al. 2011. A developmental staging table for *Astyanax mexicanus* surface fish and Pachón cavefish. Zebrafish 8:155–165.

Hinaux H, Poulain J, Da Silva C, et al. 2013. De novo sequencing of *Astyanax mexicanus* surface fish and Pachón cavefish transcriptomes reveals enrichment of mutations in cavefish putative eye genes. PLoS One 8:e53553.

Hinaux H, Blin M, Fumey J, et al. 2015. Lens defects in *Astyanax mexicanus* cavefish: evolution of *crystallins* and a role for *alphaA-crystallin*. Dev Neurobiol 75:505–521.

Hinaux H, Devos L, Blin M, et al. 2016. Sensory evolution in blind cavefish is driven by early embryonic events during gastrulation and neurulation. Development 143:4521–4532.

Inbal A, Kim S-H, Shin J, Solnica-Krezel L. 2007. *Six3* represses *nodal* activity to establish early brain asymmetry in zebrafish. Neuron 55:407–415.

Ishida Y, David VA, Eizirik E, et al. 2006. A homozygous single-base deletion in *MLPH* causes the dilute coat color phenotype in the domestic cat. Genomics 88:698–705.

Jeffery WR. 2001. Cavefish as a model system in evolutionary developmental biology. Dev Biol 231:1–12.

Jeffery WR. 2005. Adaptive evolution of eye degeneration in the Mexican blind cavefish. J Hered 96:185–196.

Jeffery WR. 2009a. Evolution and development in the cavefish *Astyanax*. Curr Top Dev Biol 86:191–221.

Jeffery WR. 2009b. Regressive evolution in *Astyanax* cavefish. Ann Rev Genet 43:25–47.

Jeffery W, Strickler A. 2003. To see or not to see: evolution of eye degeneration in Mexican blind cavefish. Integr Comp Biol 43:531–541.

Kowalko JE, Rohner N, Linden TA, et al. 2013. Convergence in feeding posture occurs through different genetic loci in independently evolved cave populations of *Astyanax mexicanus*. Proc Natl Acad Sci USA 110:16933–16938.

Kremeyer B, Lopera F, Cox JJ, et al. 2010. A gain-of-function mutation in *TRPA1* causes familial episodic pain syndrome. Neuron 66:671–680.

Lévai O, Feistel T, Breer H, Strotmann J. 2006. Cells in the vomeronasal organ express odorant receptors but project to the accessory olfactory bulb. J Comp Neurol 498:476–490.

Levy C, Khaled M, Fisher DE. 2006. MITF: master regulator of melanocyte development and melanoma oncogene. Trends Mol Med 12:406–414.

de la O Leyva-Pérez M, Valverde-Corredor A, et al. 2014. Early and delayed long-term transcriptional changes and short-term transient responses during cold acclimation in olive leaves. DNA Res 22:1–11.

Love MI, Huber W, Anders S. 2014. Moderated estimation of fold change and dispersion for RNA-seq data with DESeq2. Genome Biol 15:550.

McCurley AT, Callard GV. 2008. Characterization of housekeeping genes in zebrafish: male-female differences and effects of tissue type, developmental stage and chemical treatment. BMC Mol Biol 9:102.

McGaugh SE, Gross JB, Aken B, et al. 2014. The cavefish genome reveals candidate genes for eye loss. Nat Commun 5:5307.

Ménasché G, Ho CH, Sanal O, et al. 2005. Griscelli syndrome restricted to hypopigmentation results from a melanophilin defect (GS3) or a *MYO5A* F-exon deletion (GS1). J Clin Invest 112:450–456.

Meng F, Zhao Y, Postlethwait JH, Zhang C. 2013. Differentially-expressed *opsin* genes identified in *Sinocyclocheilus* cavefish endemic to China. Curr Zool 59:170–174.

Mitchell RW, Russell WH, Elliot WR. 1977. Mexican eyeless characin fishes, genus *Astyanax*: Environment, distribution, and evolution. Special Publications: The Museum, Texas Tech University. 12: 1–89.

Moran D, Softley R, Warrant EJ. 2014. Eyeless Mexican cavefish save energy by eliminating the circadian rhythm in metabolism. PLoS ONE 9:e107877.

Moran D, Softley R, Warrant EJ. 2015. The energetic cost of vision and the evolution of eyeless Mexican cavefish. Sci Adv 1:e1500363–e1500363.

Mortazavi A, Williams BA, Mccue K, Schaeffer L, Wold B. 2008. Mapping and quantifying mammalian transcriptomes by RNA-Seq. Nat Methods 5:621–628.

Neely GG, Keene AC, Duchek P, et al. 2011. TrpA1 regulates thermal nociception in Drosophila. PLoS ONE 6:e24343.

Oike H, Nagai T, Furuyama A, et al. 2007. Characterization of ligands for fish taste receptors. J Neurosci 27:5584–5592.

O'Quin K, Yoshizawa M, Doshi P, Jeffery W. 2013. Quantitative genetic analysis of retinal degeneration in the blind cavefish *Astyanax mexicanus*. PLoS ONE 8:e57281.

Pottin K, Hinaux H, Retaux S. 2011. Restoring eye size in *Astyanax mexicanus* blind cavefish embryos through modulation of the *Shh* and *Fgf8* forebrain organising centres. Development 138:2467–2476.

Prober DA, Zimmerman S, Myers BR, et al. 2008. Zebrafish TRPA1 channels are required for chemosensation but not for thermosensation or mechanosensory hair cell function. J Neurosci 28:10102–10110.

Protas M, Conrad M, Gross JB, Tabin C, Borowsky R. 2007. Regressive evolution in the Mexican cave tetra, Astyanax mexicanus. Curr Biol 17:452–454.

Protas ME, Hersey C, Kochanek D, et al. 2006. Genetic analysis of cavefish reveals molecular convergence in the evolution of albinism. Nat Genet 38:107–111.

Saade CJ, Alvarez-Delfin K, Fadool JM. 2013. Rod photoreceptors protect from cone degeneration-induced retinal remodeling and restore visual responses in zebrafish. J Neurosci 33:1804–1814.

Seo M, Kim K, Yoon J, et al. 2016. RNA-seq analysis for detecting quantitative trait-associated genes. Sci Rep 6:24375.

Shibahara S, Takeda K, Yasumoto KI, et al. 2001. Microphthalmia-associated transcription factor (MITF): multiplicity in structure, function, and regulation. J Investig Dermatol Symp Proc 6:99–104.

Stahl BA, Gross JB. 2015. Alterations in *Mc1r* gene expression are associated with regressive pigmentation in *Astyanax* cavefish. Dev Genes Evol 225:367–375.

Strickler A, Jeffery W. 2009. Differentially expressed genes identified by cross-species microarray in the blind cavefish Astyanax. Integr Zool 4:99–109.

Strychalski J, Gugołek A, Antoszkiewicz Z, Kowalska D, Konstantynowicz M. 2016. Biologically active compounds in selected tissues of white-fat and yellow-fat rabbits and their production performance parameters. Livest Sci 183:92–97.

Thisse B, Thisse C. 2004. Fast release clones: a high throughput expression analysis. ZFIN Direct Data Submission.

Tian R, Cullen NG, Morris CA, et al. 2012. Major effect of retinal short-chain dehydrogenase reductase (*RDHE2*) on bovine fat colour. Mamm Genome 23:378–386.

Våge DI, Boman IA. 2010. A nonsense mutation in the *beta-carotene oxygenase 2* (*BCO2*) gene is tightly associated with accumulation of carotenoids in adipose tissue in sheep (*Ovis aries*). BMC Genet 11:10.

Vincent A, Forster N, Maynes JT, et al. 2014. *OTX2* mutations cause autosomal dominant pattern dystrophy of the retinal pigment epithelium. J Med Genet 51:797–805.

Warden CD, Yuan YC, Wu X. 2013. Optimal calculation of RNA-seq fold-change values. Int J Comput Bioinfo In Silico Model 2:285–292.

Wilkens H. 1988. Evolution and genetics of epigean and cave *Astyanax fasciatus* (Characidae, Pisces). Evol Biol 23:271–367.

Wilkens H, Strecker U. 2003. Convergent evolution of the cavefish *Astyanax* (Characidae, Teleostei): genetic evidence from reduced eye-size and pigmentation. Biol J Linn Soc 80:545–554.

Wyatt A, Bakrania P, Bunyan DJ, et al. 2008. Novel heterozygous OTX2 mutations and whole gene deletions in anophthalmia, microphthalmia and coloboma. Hum Mutat 29(11):E278–E283.

Yamamoto Y, Jeffery WR. 2000. Central role for the lens in cave fish eye degeneration. Science 289:631–633.